Available on: http://gjetr.ep-journals.org/ E-ISSN: 3051-3782, P-ISSN: 3051-3774

Global Journal of Engineering and Technology Review

Volume: 02 Issue: 09 September 2026

Density Functional Theory Investigation of Defect-Induced Electronic Behavior in Iodine-Deficient Mapbi$_3$ Perovskites for Solar Cells

Sani Kado
Department of Physics Federal University Dutsin-Ma Katsina, Nigeria.

Muhammad Y. Onimisi
Department of Physics Nigerian Defense Academy Kaduna, Nigeria.

Dahiru M. Sanni
Department of Physics Federal University Dutsin-Ma Katsina, Nigeria.

Published Date: September 30, 2026 **Article DOI : 10.65150/EP-gjetr/V2E9/2026-15**

ABSTRACT: This work Demonstrated a Density Functional Theory (DFT) investigation of the electronic properties and iodine vacancy defects in methylammonium lead iodide ($MAPbI_3$) using the Vienna Ab initio Simulation Package (VASP). We analyzed the structural and electronic properties of both pristine and defective $MAPbI_3$ systems. Density of state (DOS) and band structure calculations confirmed that pristine $MAPbI_3$ is a direct-bandgap semiconductor. Our defect analysis revealed that iodine vacancies alter the electronic structure by introducing new states near the band edges. Formation energy calculations showed that the positively charged iodine vacancy (+1) possesses the lowest formation energy (0.20 eV), indicating its thermodynamic stability. The values of Charge transition levels for ε (+1/0), and ε (0/−1) were obtained as 1.12 eV and 1.52 eV respectively within the bandgap. The defect concentration analysis showed that the +1-charge state is the most stable and predominant at both 298 K and 333 K. This indicates that iodine vacancies play an important role in determining the charge transport and recombination behavior of $MAPbI_3$. Understanding these defect effects provides useful insight for optimizing the material properties and enhancing the efficiency and overall performance of perovskite solar cells.

KEYWORDS: Density Functional Theory, $MAPbI_3$, iodine vacancy, perovskite solar cells, VASP, defect formation energy

1. INTRODUCTION

Perovskite solar cells (PSCs) have emerged as one of the most promising next-generation photovoltaic technologies, demonstrating an unprecedented trajectory of efficiency improvement that has captivated the global scientific community. Based on hybrid organic-inorganic or all-inorganic halide perovskite materials characterized by the general formula ABX_3, these devices have achieved remarkable power conversion efficiencies (PCEs) that have surged from a modest 3.8% in 2009 to certified values exceeding 26% for single-junction devices and an impressive 36.1% for perovskite/silicon tandem configurations [1,2]. This extraordinary rate of progress, unparalleled in the history of solar cell development, positions PSCs as transformative candidates for addressing the escalating global energy demand while mitigating the environmental degradation associated with conventional fossil fuel-based energy sources [3].

The exceptional performance of PSCs stems from a unique confluence of intrinsic optoelectronic properties that distinguish these materials from traditional photovoltaic absorbers. Perovskites exhibit excellent light absorption capabilities, characterized by high absorption coefficients approaching 10^5 cm^{-1}, enabling ultrathin films of approximately 500 nm to efficiently capture the entire visible solar spectrum [4]. Furthermore, their direct bandgaps are highly tunable by adjusting the halide content, offering flexibility for optimization across various applications, from single-junction cells to multi-junction tandem configurations. For instance, formamidinium lead trihalide can have its bandgap tuned as low as 1.48 eV, approaching the theoretical optimum for single-junction devices [5]. Beyond light absorption, perovskites boast high charge-carrier mobilities and exceptionally long carrier diffusion lengths, often exceeding 1 μm, which are crucial for efficient charge separation and transport to the electrodes [6]. The low exciton binding energies in these materials further ensure that photogenerated electron-hole pairs are easily separated upon photon absorption, contributing to high charge generation efficiency. A unique feature observed in perovskite materials is their very slow surface recombination rate, even on passivated surfaces, which minimizes losses at interfaces [7]. Perovskites are also often described as having high defect tolerance, meaning that many intrinsic defects tend to form shallow-level defect states with low formation energies, having a negligible effect on charge carrier dynamics and non-radiative recombination [8].

Complementing these outstanding optoelectronic properties is the inherent low-cost manufacturing potential of PSCs. Their solution processability enables high-throughput fabrication techniques such as roll-to-roll printing, slot-die coating, and inkjet printing, offering a significant economic advantage over conventional silicon-based solar cells, which typically require energy-intensive, high-temperature vacuum processes [9]. This

License: This is an open access article under the CC BY 4.0 license: https://creativecommons.org/licenses/by/4.0/

unique combination of high efficiency and low-cost, scalable manufacturing positions PSCs with transformative potential for rapid terawatt-scale solar deployment, directly addressing the global energy challenge by providing an affordable and abundant renewable energy solution [10].

Despite the remarkable progress and inherent advantages, the widespread commercialization and definitive market penetration of PSCs are currently impeded by persistent challenges, primarily concerning their long-term operational stability and reproducibility under ambient conditions [11]. A fundamental origin of these issues lies in the intrinsic presence of defects within the perovskite material itself and, critically, at its interfaces with the adjacent charge transport layers (CTLs) and electrodes. These defects act as highly efficient non-radiative recombination centres for photogenerated electron-hole pairs, diverting charge carriers from contributing to electrical current and consequently limiting key photovoltaic parameters such as the open-circuit voltage (V_{oc}), short-circuit current density (J_{sc}), and fill factor (FF) [12]. The reduction in these parameters directly translates to a diminished overall PCE of the device. For instance, increasing the defect density in the $CH_3NH_3PbI_3$ absorber layer from 2.5×10^{15} cm^{-3} to 2.5×10^{18} cm^{-3} can cause the PCE to drop from 17.60% to 0.86%, demonstrating a highly non-linear response where performance remains relatively stable below a critical defect density but collapses rapidly once that threshold is exceeded [13].

Beyond efficiency losses, the soft ionic nature and low defect formation energy of perovskites render them susceptible to the formation and migration of mobile ionic defects. These mobile ions, such as halide anions and organic cations, readily migrate when subjected to operational stressors like illumination, elevated temperatures, or external electric biases [14]. The accumulation of these charged defects at interfaces and within the bulk perovskite layer contributes to anomalous current-voltage (J-V) hysteresis, a phenomenon that complicates accurate device characterization and performance evaluation. For instance, iodine vacancy (V_i) conduction is identified as a primary cause of J-V hysteresis, with diffusion coefficients estimated at 3-6 $\times$ 10^{-13} cm^2/s, consistent with density functional theory (DFT) predictions [15]. More critically, this ion migration is a primary driver of intrinsic instability, triggering chemical reactions, phase segregation, and macroscopic defect growth, thereby accelerating the degradation of the perovskite material and the charge transport layers over time [16]. This complex feedback loop, where intrinsic material properties and extrinsic operational conditions conspire to generate and activate defects, represents a major impediment to the long-term reliability of PSCs [17].

The quality of the interfaces within a PSC device, including precise energy level alignment and efficient charge extraction, is paramount for achieving and maintaining high performance and stability. Poorly engineered interfaces can exacerbate recombination, hinder charge collection, and provide pathways for external degradants like moisture and oxygen to penetrate the active layer, leading to accelerated device degradation [18]. The intricate interplay between defect-related phenomena and interfacial properties underscores the need for a deeper, more fundamental understanding to unlock the full potential of PSC technology [19]. Theoretical and computational modelling, ranging from atomistic simulations (such as DFT and molecular dynamics) to mesoscopic (kinetic Monte Carlo) and device-level (drift-diffusion) simulations, offers a powerful and indispensable complementary tool to experimental characterization techniques [20]. These computational approaches can provide microscopic insights into defect formation energies, ion migration barriers, charge carrier dynamics, and interfacial energy alignment that are often inaccessible or challenging to probe experimentally [21,22]. By providing a predictive framework, theoretical modelling can guide rational device design, accelerate materials discovery, and ultimately bridge the gap between fundamental scientific understanding and the practical engineering of efficient and stable PSCs for commercial deployment [23].

This research presents a comprehensive theoretical investigation employing DFT calculations using the Vienna Ab initio Simulation Package (VASP) to systematically investigate the impact of iodine vacancy defects on the electronic properties and stability of methylammonium lead iodide ($MAPbI_3$), a prototypical perovskite material. The study examines the defect formation energies, charge transition levels, and defect concentrations for different charge states of iodine vacancies, providing critical insights into the thermodynamic stability and electronic behaviour of these defects under various conditions. By elucidating the fundamental relationships between atomic-scale defects and device performance, this work contributes to the development of more efficient, stable, and scalable PSC technologies.

2. COMPUTATIONAL METHODOLOGY

2.1 Density Functional Theory Calculations

First-principles calculations were performed using Density Functional Theory (DFT) as implemented in the Vienna Ab initio Simulation Package (VASP). The calculations were carried out to investigate the electronic properties and iodine vacancy defects in methylammonium lead iodide ($MAPbI_3$) perovskite. DFT provides a reliable framework for describing the electronic structure and defect energetics of semiconductor materials at the atomic

The pristine $MAPbI_3$ crystal structure was initially optimized through full structural relaxation to obtain the equilibrium lattice parameters and atomic coordinates corresponding to the minimum total energy configuration. During geometry optimization, all atomic positions were allowed to relax until the convergence criteria for total energy and atomic forces were satisfied. The optimized structure served as the reference system for subsequent defect calculations.

To accurately describe the interaction between the organic methylammonium ($CH_3NH_3^+$) cation and the inorganic PbI_3 framework, van der Waals corrections were incorporated during the calculations. Scalar-relativistic pseudopotentials were employed to account for relativistic effects associated with the heavy lead atoms present in the perovskite structure. In addition, spin–orbit coupling (SOC) effects were considered during electronic structure calculations because SOC significantly influences the conduction band characteristics of lead-based halide perovskites.

2.2 Supercell Construction and Defect Modelling

Following optimization of the primitive unit cell, a 2 × 2 × 2 supercell was constructed to model isolated point defects while minimizing interactions between periodic images. The larger supercell provides a more realistic representation of dilute defect concentrations commonly observed in experimental systems.

An iodine vacancy (V_i) was introduced by removing one iodine atom from the optimized supercell. The defective structure was subsequently relaxed to allow neighbouring atoms to adjust to the absence of the iodine atom. This relaxation process accounts for local lattice distortions induced by defect formation and ensures that the defective configuration corresponds to its lowest-energy state.

License: This is an open access article under the CC BY 4.0 license: https://creativecommons.org/licenses/by/4.0/

Corresponding Author: Sani Kado

Different charge states of the iodine vacancy were investigated to determine their thermodynamic stability and electronic characteristics. Total energies of both pristine and defective structures were obtained for subsequent defect formation energy calculations.

2.3 Electronic Structure Analysis

The electronic properties of pristine and defective $MAPbI_3$ were evaluated through band structure and density of states (DOS) calculations. Self-consistent field (SCF) calculations were first performed to obtain converged charge densities, followed by non-self-consistent field (NSCF) calculations along high-symmetry k-point paths within the Brillouin zone.

The total and projected density of states were analysed to determine the orbital contributions of constituent atoms to the valence and conduction bands. Comparison between pristine and defective systems enabled identification of defect-induced electronic states and their influence on the bandgap region. Particular attention was given to localized states introduced by iodine vacancies that may act as carrier trapping or recombination centres.

2.4 Defect Formation Energy Calculations

The thermodynamic stability of iodine vacancies was quantified through defect formation energy calculations. The formation energy of a defect in charge state q was calculated using:

$$E_f(D^q) = E_T(D^q) - E_T(bulk) - \sum_i n_i\mu_i + qE_F \qquad (2.4)$$

Formation energies were evaluated over the entire bandgap range to determine the most stable charge state under different electronic conditions.

2.5 Charge Transition Levels

Charge transition levels were calculated to determine the Fermi level positions at which the iodine vacancy changes its charge state. These transition levels provide information regarding the donor or acceptor behaviour of the defect and its ability to participate in carrier trapping processes.

The charge transition level between two charge states (q) and (q') was obtained from:

$$\varepsilon\left(\frac{q}{q'}\right) = \frac{E_f(D^q) - E_f(D^{q'})}{q' - q} \qquad (2.5)$$

he resulting transition levels were analyzed relative to the valence band maximum and conduction band minimum to classify the defect as shallow or deep within the bandgap.

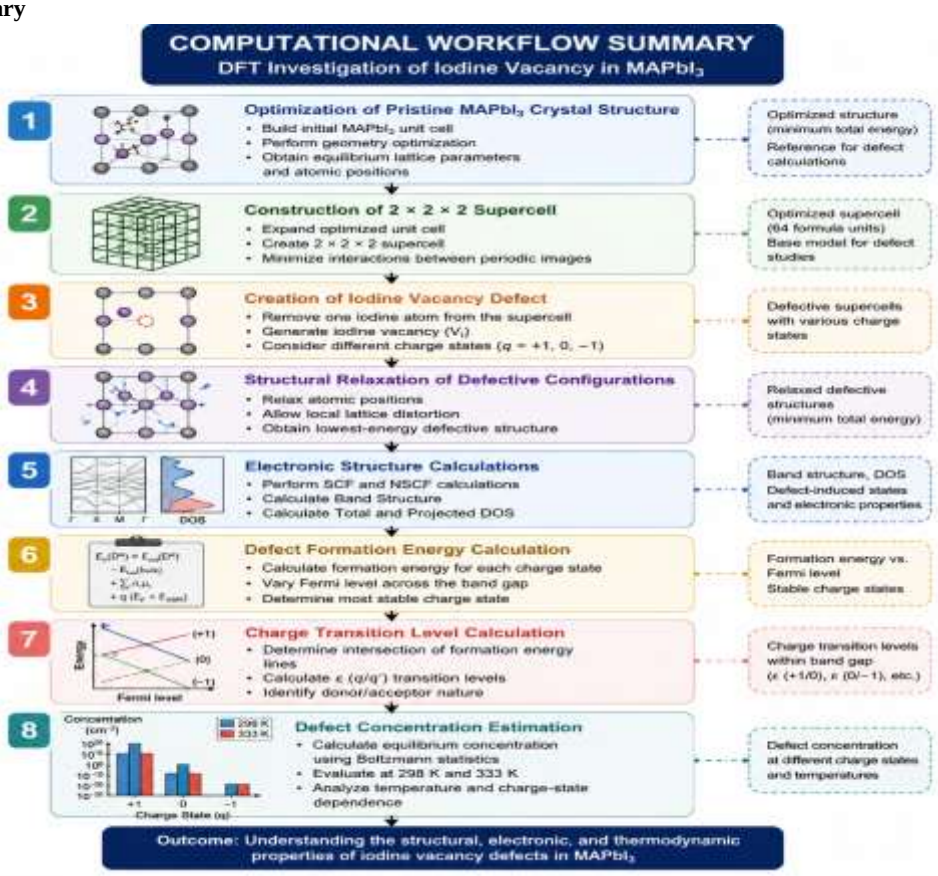
2.6 Defect Concentration Analysis

The equilibrium concentration of iodine vacancies was estimated using Boltzmann statistics:

$$N_D = N_{sites}\, exp\left(-\frac{E_f}{k_B T}\right) \qquad (2.6)$$

Defect concentrations were calculated at room temperature (298 K) and typical solar-cell operating temperature (333 K) to evaluate the thermal stability and prevalence of various charge states under practical operating conditions.

2.7 Workflow Summary



License: This is an open access article under the CC BY 4.0 license: https://creativecommons.org/licenses/by/4.0/

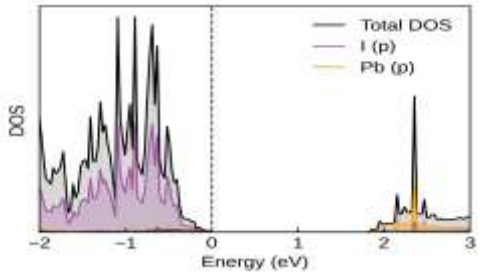
This systematic approach enables a comprehensive understanding of the structural, electronic, and thermodynamic properties of iodine vacancy defects in $MAPbI_3$ and their influence on perovskite solar-cell performance.

3. RESULTS AND DISCUSSION

3.1 Electronic Properties of Pristine $MAPbI_3$

3.1.1 Density of States and Band Structure

The calculated Density of States (DOS) and band structure confirmed that pristine $MAPbI_3$ exhibits semiconducting behaviour with a direct band gap. The absence of electronic states around the Fermi level indicates good electronic stability and suitability for photovoltaic applications.
The valence band was mainly composed of iodine-derived orbitals, while the conduction band was dominated by lead orbitals, suggesting efficient electronic transition and charge transport.



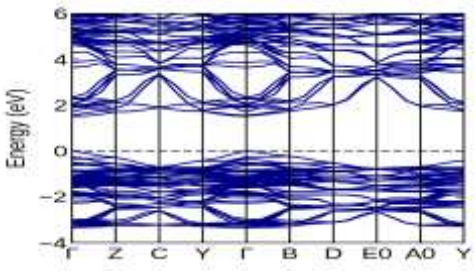


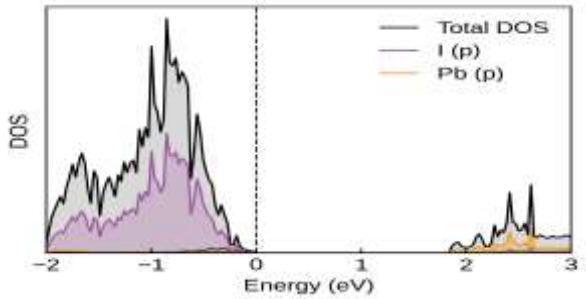
Figure 3.1 (a) Density of States (DOS) of pristine $MAPbI_3$ **Figure 3.1 (b) Band structure of pristine $MAPbI_3$**

The calculated band gap of approximately 1.8–2.0 eV agrees reasonably with reported DFT values and validates the computational approach.

3.2 Effect of Iodine Vacancy on Electronic Structure

3.2.1 Defective $MAPbI_3$

Introduction of iodine vacancy altered the electronic structure of $MAPbI_3$ by generating localized electronic states near the band edges. Compared with the pristine structure, the defective supercell showed band distortion and redistribution of DOS peaks, indicating disruption of Pb–I interactions. These vacancy-induced states may function as carrier trapping centres and increase non-radiative recombination losses.



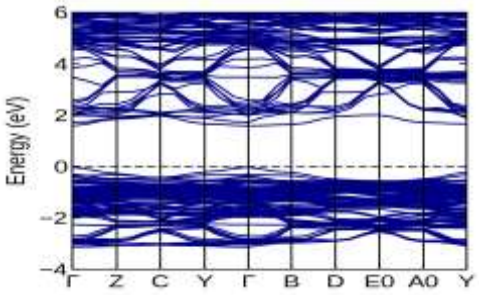


Figure 3.2.1(a) DOS of defective $MAPbI_3$ **Figure 3.2.1(b) Band of defective $MAPbI_3$**

In summary, iodine vacancies significantly modify the electronic behavior of $MAPbI_3$ by introducing localized defect states within or near the band-gap region, which disrupt the ideal electronic structure of the pristine material. The formation of these defect-induced states alters charge distribution and affects the movement of photogenerated carriers across the perovskite layer. As a result, iodine vacancies may act as carrier trapping and recombination centers, reducing carrier lifetime and limiting efficient charge extraction.

3.3 Defect Formation Energy

Table 1 summarizes the calculated defect formation energies.

Table 1. Formation energy of iodine vacancy

Charge State (q)	Formation energy (eV)	Fermi Level Range (eV)
+1	0.20	$E_F < 1.12$
0	1.32	$1.12 \leq E_F \leq 1.52$
-1	2.84	$E_F > 1.52$

License: This is an open access article under the CC BY 4.0 license: https://creativecommons.org/licenses/by/4.0/

Corresponding Author: Sani Kado

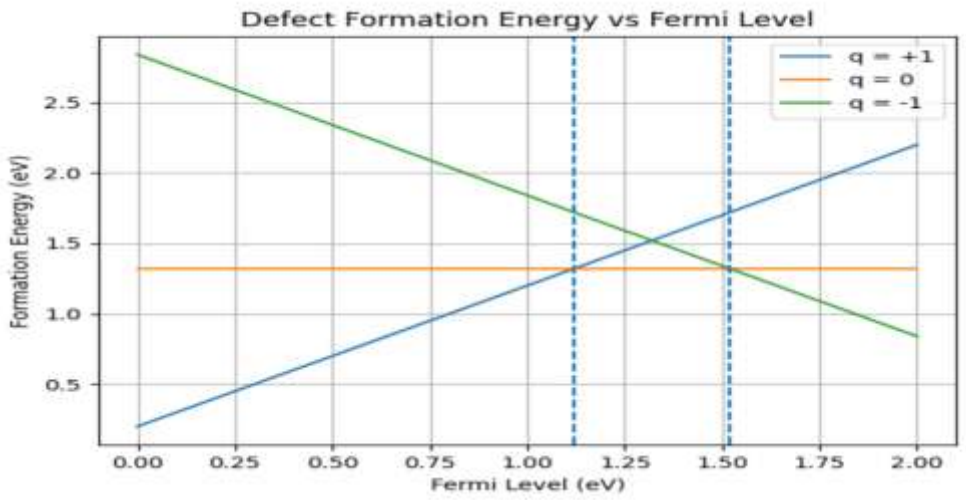


Figure 3.3. Defect formation energy versus Fermi level

The +1-charge state possesses the lowest formation energy and therefore represents the most stable defect configuration. The −1 state exhibits the highest formation energy and is least likely to occur. This behaviour indicates that iodine vacancies favour positively charged conditions and may contribute to charge imbalance during device operation.

3.4 Charge Transition Levels

The transition levels reveal the electrical activity of iodine vacancies.

Table 2. Charge transition levels

Transition	Energy Level (eV)	Position Relative to band gap	Trap Type
ε (+1/0)	1.12	Within bandgap (near mid-gap)	Acceptor-like transition
ε (0/−1)	1.52	Within bandgap (closer to CBM)	Deep acceptor level
ε (+1/−1)	1.32	Within bandgap (mid-gap region)	Negative-U behaviour

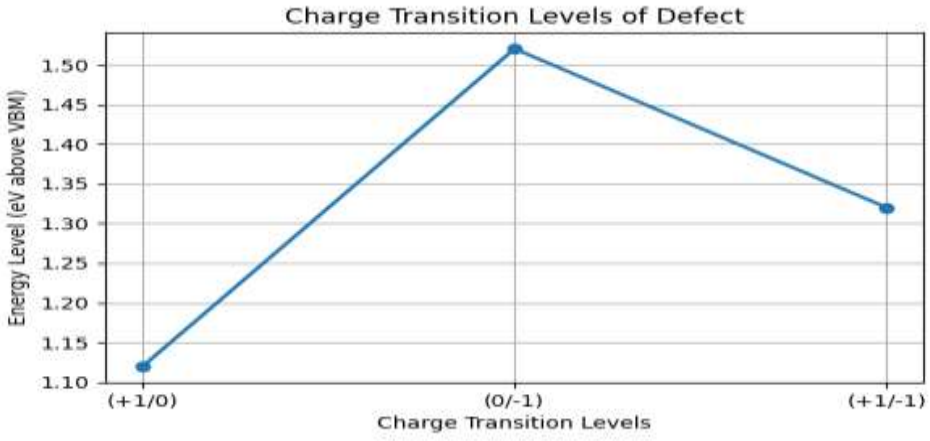


Figure 3.4 Charge transition levels for iodine vacancy

The transition ε (+1/0) appears deep inside the band gap and may act as an efficient recombination centre by capturing photogenerated electrons or holes before they contribute to electrical current generation. Deep-level defects generally reduce carrier lifetime and increase non-radiative recombination losses, which negatively affect photovoltaic efficiency. In contrast, the ε (0/−1) transition occurs closer to the conduction band, indicating relatively weaker trapping behaviour and a lower tendency to severely interrupt charge transport.

These results suggest that iodine vacancies influence both carrier transport and recombination processes in $MAPbI_3$. The presence of these transition levels can alter charge-carrier dynamics, reduce charge collection efficiency, and contribute to energy losses within the device. In addition, defect-assisted recombination may accelerate performance degradation under operating conditions, emphasizing the importance of minimizing iodine vacancy formation to achieve improved efficiency and long-term stability of perovskite solar cells.

3.5 Defect Concentration

Defect concentration was evaluated at room temperature (298 K) and operating temperature 333K

License: This is an open access article under the CC BY 4.0 license: https://creativecommons.org/licenses/by/4.0/

Table 3. Defect concentration of iodine vacancy

Charge State (q)	Formation Energy (eV)	Concentration at 298 K (cm^{-3})	Concentration at 333 K (cm^{-3})
+1	0.20	4.2×10^{18}	1.3×10^{19}
0	1.32	1.1×10^{0}	1.2×10^{3}
−1	2.84	2.5×10^{-26}	3.4×10^{-19}

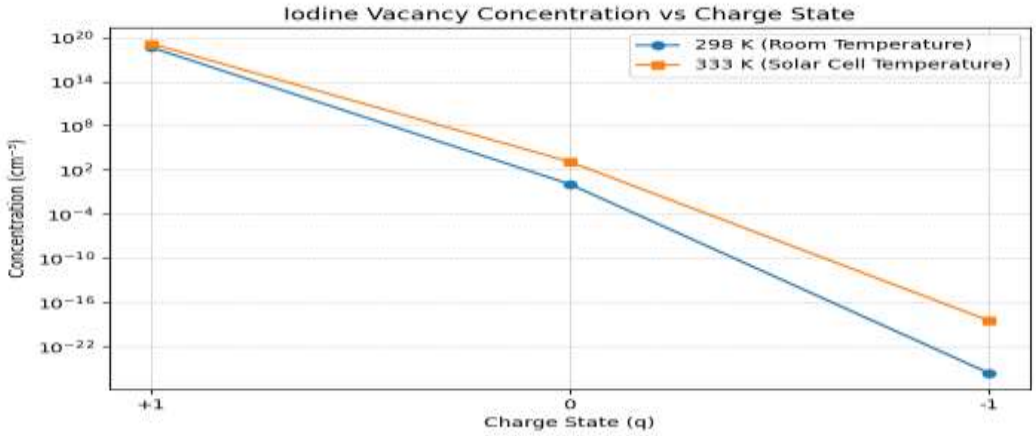


Figure 3.5. Defect concentration plot

The results show that the +1-charge state dominates at both temperatures, indicating strong thermodynamic stability. Increasing temperature slightly increases defect concentration due to thermal activation, but the relative stability order remains unchanged.

3.6 Summary of Results

The DFT calculations demonstrated that pristine $MAPbI_3$ possesses favourable semiconducting properties suitable for solar-cell applications. Introduction of iodine vacancies generated defect states near the band gap and altered electronic behaviour. Formation-energy analysis showed that the +1-charge state is the most stable configuration, while charge transition calculations revealed defect levels capable of promoting carrier recombination. Defect concentration calculations further confirmed that positively charged iodine vacancies dominate under practical operating conditions and therefore play an important role in determining the performance and stability of $MAPbI_3$ perovskite solar cells.

4. CONCLUSION

This study employed Density Functional Theory (DFT) calculations in VASP to investigate the electronic properties and iodine vacancy defects in methylammonium lead iodide ($MAPbI_3$) for perovskite solar-cell applications. The results confirmed that pristine $MAPbI_3$ exhibits favourable semiconducting characteristics with a direct band gap and electronic properties suitable for efficient photovoltaic performance.

The introduction of iodine vacancies significantly altered the electronic structure by generating localized defect states near the band-gap region. These defect-induced states modified charge transport behaviour and created potential carrier trapping and recombination centres that may reduce device efficiency.

Defect formation energy analysis revealed that the +1-charge state is the most thermodynamically stable configuration, while charge transition level calculations showed the presence of deep defect states capable of promoting non-radiative recombination. Defect concentration calculations further demonstrated that positively charged iodine vacancies dominate at both 298 K and 333 K, indicating their strong influence under practical operating conditions.

The findings show that iodine vacancies play a critical role in determining the electronic performance and stability of $MAPbI_3$. Therefore, effective control of defect formation through defect engineering and passivation strategies is essential for improving the efficiency and long-term reliability of perovskite solar cells. This study provides theoretical insight into defect behaviour and supports future optimization of $MAPbI_3$-based photovoltaic materials.

REFERENCES

1) Kojima, A., Teshima, K., Shirai, Y., & Miyasaka, T. (2009). Organometal halide perovskites as visible-light sensitizers for photovoltaic cells. Journal of the American Chemical Society, 131(17), 6050-6051.
2) National Renewable Energy Laboratory (NREL). (2024). Best research-cell efficiency chart. https://www.nrel.gov/pv/cell-efficiency.html
3) International Energy Agency (IEA). (2023). World Energy Outlook 2023. Paris: IEA Publications.
4) Green, M. A., Ho-Baillie, A., & Snaith, H. J. (2014). The emergence of perovskite solar cells. Nature Photonics, 8, 506-514.
5) Eperon, G. E., Stranks, S. D., Menelaou, C., Johnston, M. B., Herz, L. M., & Snaith, H. J. (2014). Formamidinium lead trihalide: A broadly tunable perovskite for efficient planar heterojunction solar cells. Energy & Environmental Science, 7(3), 982-988.
6) Stranks, S. D., Eperon, G. E., Grancini, G., Menelaou, C., Alcocer, M. J. P., Leijtens, T., ... & Snaith, H. J. (2013). Electron-hole diffusion lengths exceeding 1 micrometer in an organometal trihalide perovskite absorber. Science, 342(6156), 341-344.

License: This is an open access article under the CC BY 4.0 license: https://creativecommons.org/licenses/by/4.0/

Corresponding Author: Sani Kado

7) Yang, Y., Yang, M., Li, Z., Crisp, R., Zhu, K., & Beard, M. C. (2015). Comparison of recombination dynamics in $CH_3NH_3PbI_3$ and $CH_3NH_3PbBr_3$ perovskite films: Influence of exciton binding energy. Journal of Physical Chemistry Letters, 6(23), 4688-4692.
8) Yin, W. J., Shi, T., & Yan, Y. (2014). Unusual defect physics in $CH_3NH_3PbI_3$ perovskite solar cell absorber. Applied Physics Letters, 104(6), 063903.
9) Snaith, H. J. (2013). Perovskites: The emergence of a new era for low-cost, high-efficiency solar cells. Journal of Physical Chemistry Letters, 4(21), 3623-3630.
10) Park, N. G., Zhu, K., & Miyasaka, T. (2020). Perovskite solar cells: From the laboratory to the assembly line. Chemical Reviews, 120(15), 7867-7918.
11) Correa-Baena, J. P., Saliba, M., Buonassisi, T., Grätzel, M., Abate, A., Tress, W., & Hagfeldt, A. (2017). Promises and challenges of perovskite solar cells. Science, 358(6364), 739-744.
12) Abbas, G., Xu, W., Rauf, M., & Kyaw, A. K. K. (2024). A comprehensive review on defects-induced voltage losses and strategies toward highly efficient and stable perovskite solar cells. Photonics, 11(1), 87.
13) Guo, Y., Yuan, Y., Wang, Z., Zhang, J., & Zhou, Y. (2024). Understanding defects in perovskite solar cells through computation: Current knowledge and future challenges. Advanced Science, 11(16), 2305799.
14) Eames, C., Frost, J. M., Barnes, P. R. F., O'Regan, B. C., Walsh, A., & Islam, M. S. (2015). Ionic transport in hybrid lead iodide perovskite solar cells. Nature Communications, 6, 7497.
15) Azpiroz, J. M., Mosconi, E., Bisquert, J., & De Angelis, F. (2015). Defect migration in methylammonium lead iodide and its role in perovskite solar cell operation. Energy & Environmental Science, 8(7), 2118-2127.
16) Zhao, Y., et al. (2018). Interface engineering in perovskite solar cells: A theoretical approach. Advanced Energy Materials, 8(16), 1800732.
17) Snaith, H. J. (2018). Present status and future prospects of perovskite photovoltaics. Nature Materials, 17(5), 372-376.
18) Kymakis, E., Stratakis, E., & Kalyvas, N. (2018). Interfacial engineering of perovskite solar cells for improved performance and stability. Advanced Materials Interfaces, 5(22), 1801595.
19) Walsh, A., et al. (2018). Computational investigation of perovskite solar cells. Journal of Materials Chemistry C, 6(2), 321-330.
20) Yin, J., et al. (2020). Multi-scale modelling of charge transport in perovskite solar cells. Energy & Environmental Science, 13(6), 1627-1638.
21) Mosconi, E., et al. (2016). First-principles modelling of perovskite solar cells: Understanding the role of defects. Physical Review Applied, 6(4), 044012.
22) Kim, J., et al. (2019). Interface engineering for high-efficiency perovskite solar cells. Journal of Materials Chemistry A, 7(23), 14245-14253.
23) Bach, U., et al. (2019). Defects and interfaces in perovskite solar cells: A theoretical perspective. Nature Energy, 4(9), 738-746.

License: This is an open access article under the CC BY 4.0 license: https://creativecommons.org/licenses/by/4.0/

Corresponding Author: Sani Kado